A New Method to Acquire *m* Exponent and Tortuosity Factor for Microscopically Heterogeneous Carbonates, an Example from Oligo-Miocene Asmari Formation, Southwest Iran

Rezaee[1*] M.R., Motiei[2], H., and Kazemzadeh[3], E.,

1- *University of Tehran, University College of Science, School of Geology, mrezaee@khayam.ut.ac.ir*
2- *Head of Technology Division of R&D, NIOC.*
3- *Research Institute of Petroleum Industry/NIOC,*

Abstract

Many factors control accurate determination of water saturation (*Sw*). Cementation exponent (*m*) and tortuosity factor (*a*) are from those that have been focus of many studies. Log-log plot of porosity (ϕ) versus formation factor (*F*) is used to determine *m* and *a*. The cementation exponent is determined from the negative slope of the least square fit straight line of the plotted points, while the tortuosity factor is the intercept of the line where $\phi = 1$. In heterogeneous carbonate reservoirs where pores and pore throat networks are complex due to various diagenetic processes, *F* and ϕ scatter significantly on the ϕ-*F* plot. This will cause a small coefficient of determination between *F* and ϕ and thus less reliable *m* and *a*. Although classification of data based on petrofacies and/or permeability may improve the correlation to some extent, but data still show significant scatter.

Introducing current zone indicator (*CZI*) and electrical flow unit (*EFU*), this study has established a new approach to classify ϕ and *F* data. The approach enables one to obtain more accurate *m* and *a* and thus more realistic calculation of *Sw*. This study also shows forcing *a* to any fixed value, will lead to both optimistic and pessimistic estimation of *Sw* within a reservoir.

Keywords: *cementation exponent, tortuosity factor, electrical flow unit, formation factor, water saturation, carbonates.*

* Academic Visitor at School of Geology and Geophysics, University of Oklahoma, USA.
Email: mrezaee@gcn.ou.edu

1. Introduction

Estimation of water saturation (*Sw*) is one of the most important tasks in formation evaluation. Accurate estimation of *Sw* and thus hydrocarbon reserve is critical to reduce the uncertainty of financial forecasting and in developing an oil or gas field. *Sw* is a parameter that mainly should be estimated using resistivity log data. The basis for this is the conductivity difference between formation water and hydrocarbons.

Archie in 1942 studied the resistivities of a large number of brine-saturated cores recovered from various sandy formations and covering a range of porosity from 10 to 40 percent. He defined the formation resistivity factor (*F*):

$$F = R_o / R_w \tag{1}$$

Where *Ro* is the resistivity of clean, porous, water saturated formation and *Rw* is the resistivity of the formation water. Archie (1942) determined that there was also a relationship between the formation resistivity factor and the porosity and permeability of the reservoir rock. He defined the following relationship with porosity:

$$F = \phi^{-m} \tag{2}$$

where ϕ and *m* are porosity and cementation exponent respectively.

Later the formation factor was slightly modified by Winsauer et al., (1952). They measured formation factors of 29 highly varied sandstone samples. They generalized Archie's equation to:

$$F = \frac{a}{\phi^m} \tag{3}$$

where *a* is tortuosity factor.

Archie also summarized the work of earlier workers showing the relationship between water saturation and the R_t / R_o ratio and this lead to the development of the Archie's equation for the *Sw* estimation in clean formations:

$$S_w = \left(\frac{aR_w}{\phi^m R_t}\right)^{1/n} \quad (4)$$

where *Rt* is true resistivity of the formation and *n* is saturation exponent.

The accuracy of *Sw* calculation depends on the accuracy of the Archie's parameters, *a*, *m* and *n*. These parameters, that can not be measured experimentally, have been subject of many studies. It has been shown that the use of inaccurate values for Archie's parameters have significant effects on *F* and thus on *Sw* calculation (Hosseini-nia and Rezaee, 2002).

In routine formation evaluation *m* and *a* are considered constant for a given reservoir rock. It is a common practice to obtain *m* by assuming a constant value for *a* and calculating *m* for each sample. Rocks, mainly carbonates, display complex pore structures, which significantly affect their electrical resistivity. Since physical properties of these rocks may vary significantly from one sample to another, *m* and *a* values can not be considered constant.

In this paper, a new method has been introduced to classify *F* and porosity into separate electrical flow units (*EFU*), using current zone indicator (*CZI*). The method improves porosity and *F* correlation considerably.

This study also shows that forcing *a* to be a constant value causes *m* to increase. Consequently, this will lead to both pessimistic and optimistic calculation of *Sw*, depending on the reservoir tortuosity factor.

2. Basic Concepts

2.1 Cementation exponent

Cementation exponent was first defined by Archie in 1942. Noticing that an increase in *m* values is associated with sandstone consolidation, Archie named this exponent as cementation exponent. A wide range of *m* values has been introduced by several authors ranging from 1 for fractured rocks to slightly more than 5 for highly compacted rocks. In Archie's study (1942), *m* was 1.3 for unconsolidated sands and ranged between 1.8 and 2.0 for cemented sandstones. Timur et al., (1972) obtained values of $a = 1.13$ and $m = 1.73$ for 1800 sandstones from 15 oil fields. Wong *et al.* (1984) worked on fused-glass

beads and showed that *m* values were 2.3 for $0.02<\phi<0.2$, and 1 for $0.2<\phi<0.4$. Hamada et al., (2002) determined values of *a* and *m* for 20 clean and porous sandstones. They found *a* and *m* being 1.36 and 2.03 for one well, and 0.95 and 1.85 for the second well, respectively. Focke and Munn (1987) demonstrated that *m* depended on the petrofacies and porosity type in carbonates. In their study, assuming $a=1$, *m* ranged between 2 and values as high as 5.5. Dubois et al., (2001) introduced $m=1.36$ for oomoldic limestones.

Using Archie's Equation as a base, many authors (e.g., Neustaedter, 1968; Nugent et al., 1978; Sethi, 1979; Rasmus, 1983; Borai, 1987; Focke and Munn, 1987) have introduced methods to determine *m from* log data. Log porosity and invasion corrected deep resistivity (Ro) were used to estimate *F* in wet zone. In all mentioned studies, *a* was assumed 1.

2.2 Tortuosity Factor

The tortuosity (*a*) has been theoretically defined as the ratio of the mean path length (*La*) to the straight line of porous medium length (*L*) (Carman, 1937):

$$a = La / L \qquad (5)$$

A value of 25/12 was determined for the tortuosity of uniform spherical particles by Bird et al., (1960) using Blake-Kozeny model. Higher values of tortuosity have been reported by many researchers. Wong *et al.* (1984) showed that tortuosity became 3.3 when ϕ was between 0.02 and 0.2 in fused-glass beads. Dubois et al., (2001) found tortuosity factor of about 9.5 for oomoldic limestones. Hirasaki (2005) reported an increase in tortuosity when sorting (standard deviation of grain size) and porosity of sand grains decreased. He showed that *a* value could reach 35 when porosity of sand grains approach zero due to sorting reduction. Attia (2005) suggested that tortuosity factor could not be considered constant since it depended on many factors such as the amount of fine grains, formation resistivity factor, cementation exponent, porosity and degree of brine saturation.

In general, the more tortuous the pore throats are, the harder it is for current to flow through the reservoir and the higher the resistivity.

3. Inter-relationship of *m* and *a*, Theoretical Derivation

Wyllie and Rose (1950) mentioned a 100-fold increase in *a* was accompanied by a 4-fold increase in *m.* Salem and Chilingarian (1999) suggested that 10-fold increase in *a* lead to a 4-fold increase in *m.* They also introduced the following empirical equation:

$$m = 1.5551 + 2.1039 \log a \qquad (6)$$

Despite of reported links between *m* and *a* by several authors, this study suggests that there is no direct relationship between *a* and *m.* They have different nature which could not be compared. *a* refers to tortuosity of pore throats whereas *m* defines degree of pores connectivity (Rezaee, in prep.). Tortuosity may vary from one sample to another without any change in *m* and vise versa. One can not compare *m* and *a* with each other, but can evaluate their influence on *F*. In Table 1 formation factors of rocks with different *m*, *a*, and porosity values are calculated using Equation 3 to evaluate the relationship among *F*, *m* and *a*.

Considering a constant value for *m* (e.g., *m*=2), Table 2 shows tortuosity factors calculated from Equation 3 ($a = F\phi^2$) using *F* values in Table 1. It can be seen that *a* increases as *F* values increase, and it is more pronounced in low porosity samples.

Figure 1 is a cross-plot of porosity versus *a* values of Table 2. It indicates a power law relationship between the two variables (Equations in Table 2). In each equation, the exponents and intercepts are m_2-m_1 and a_1, respectively. m_1 and a_1 refer to *m* and *a* values in Table 1 used to calculate *F*, m_2 was considered 2. It can be concluded that to remain *F* values unchanged, when *m* changes, tortuosity factor must be adjusted according to the following general equation:

$$a_2 = a_1 \phi^{\Delta m} \qquad (7)$$

where Δm is m_2-m_1.

As an example, for a rock with a porosity value of 10%, *m* = 2.4 and *a* = 1.3, *F* will be 326.545 (Table 1). Again, for such a rock, with a presumed constant formation factor of 326.545 and a value of 2 for *m*, *a* must be adjusted to a value of 3.265.

Back to Equation 3, in order to know how F varies for a rock with a given porosity, if m changes from m_1 to m_2 and a from a_1 to a_2, F is:

$$F = \frac{a_2}{\phi^{m2}} \tag{8}$$

or

$$F = \frac{a_1}{\phi^{m1}} \tag{9}$$

if a_2 in Equation 8 is substituted with a_2 in Equation 7 then:

$$F = a_1 \frac{\phi^{\Delta m}}{\phi^{m2}} \tag{10}$$

Equation 7 can be rearranged as:

$$a_1 = a_2 \phi^{-\Delta m} \tag{11}$$

and, if a_1 in equation 9 *is* substituted with a_1 in equation 11, then:

$$F = a_2 \frac{\phi^{-\Delta m}}{\phi^{m1}} \tag{12}$$

Equation 12 can be rearranged as follow:

$$a_2 = \frac{F\phi^{m1}}{\phi^{-\Delta m}} \tag{13}$$

Equations 8 and 9 show the inter-relationships among porosity, F, a, and m values. As an example, in a rock with 15% porosity, m_1=1.2 and a_1=14, F will be 77.94. If m and a change to m_2=2.2 and a_2=1.2, with the same porosity, then F will be 136.4.

In Equations 10 and 12, F will vary following changes in either a or m. When porosity and F remain unchanged, but m values change, a can be calculated using Equation 13. For example, in a rock with given values of porosity=15%, *a=14*, *m=1.2* and F=136.4, if m changes from 1.2 to 2.2, a will be 2.1.

To calculate *m,* Equation 13 can be rearranged as follow:

$$a_2 \phi^{-\Delta m} = F\phi^{m1} \tag{14}$$

Taking logarithm from both sides of Equation 14:

$$\log a_2 - \Delta m \log \phi = \log F + m_1 \log \phi \tag{15}$$

and rearranging Equation 15 to:

$$-\Delta m \log \phi = \log F + m_1 \log \phi - \log a_2 \tag{16}$$

the following equation can be obtained :

$$\Delta m = -\frac{\log F + m_1 \log \phi - \log a_2}{\log \phi} \tag{17}$$

since $\Delta m = m_2 - m_1$, then m_2 is calculated as:

$$m_2 = [-\frac{\log F + m_1 \log \phi - \log a_2}{\log \phi}] + m_1 \tag{18}$$

Equation 18 is a theoretical derivation of Equation 13, to calculate changes in *m* values when *a* is varied for a given sample.

Although in these equations, *m* and *a* are related, it does not necessarily mean that there is a direct relationship between *a* and *m*, as other authors reported, since *F* is involved in all equations. These equations will enable us, in the following sections, to evaluate errors generated for *Sw* calculation, when forcing *a* to any fixed values.

4. Studied Samples Characteristics

In this study, 92 clean carbonate core samples were selected from Asmari Formation in six wells of three oil fields, Zagros Basin, southwest Iran. Oligo-Miocene Asmari Formation is one of the most important carbonate oil reservoirs in Zagros Basin. Microfacies analysis of the samples examined by Maghsoodi and Rezaee (2005) showed that Asmari Limestone deposited mainly in a carbonate inner ramp. Petrographic studies indicated eight petrofacies in the samples. These petrofacies included dolomicrite, dolomitized packstone-grainstone, dolostone, sandy dolostone, grainstone, packstone, wackstone and mudstone. Mechanical and chemical compaction, extensive cementation,

selective dissolution and pervasive dolomitization were major diagenetic processes affecting original texture of the formation. Dolomitization was a common feature in most samples and in many cases was completely overprinted the original texture. Most of dolomite crystals varied in size from medium to micrite resulting in very fine pores and pore throats. Original pore spaces were mainly occluded by different generation of calcite and anhydrite cements. Porosity of the samples was generally fine intercrystalline, vugs and moldic. In most samples, no connected visible porosity could be seen (Maghsoodi and Rezaee, 2005).

4.1 Core Analysis

Selected samples were cleaned by toluene in a Soxhlet apparatus, and dried at 60°C for 24 hours prior to any analysis. Porosity and permeability were measured in reservoir condition using Ultra-Porosimeter 200A, Ultra-Permeameter and CMS-300™ (Core Measurement System). Core porosity values ranged from 2.5 to 26% with a mean value of 10%. Range of permeability was between 0.01 and 91.9mD with a mean value of 5.4 mD.

In order to measure electrical resistivity (*Ro),* samples were fully saturated by a brine with approximately the same water salinity of Asmari Formation (200,000 ppm, NaCl). Using FRF Overburden Rig at a frequency of 1kHz, electrical resistance (*r*) of the samples was measured along the axis of cylindrical plugs in reservoir condition. Then, resistivity (*R*) was calculated from the measured resistance (*r*) using the cross-sectional area of the core (*A*) and the length of the core (*L*). Formation factor was obtained as a ratio of rock resistivity (*Ro*) to brine resistivity (*Rw*). It ranged from 24 to 1611 with a mean value of 206.

4.2 Determination of m and a

The conventional determination of *m* and *a* is based on Equation 3 that can be rewritten as:

$$\log F = \log a - m \log \phi \tag{19}$$

This equation indicates that log-log plot of F versus ϕ can be used to determine a and m. The cementation exponent m, is negative slope of the least square fit straight line of the plotted points, while the tortuosity factor is the intercept of the line at $\phi = 1$. Figure 2 shows log-porosity versus log formation factor for the samples of this study. Two different methods were applied to obtain m and a (Figure 2). The first was to use a free best fit line (continuous line). The slope of this free fit line is -0.94 and intercept is 14.34 with a coefficient of determination of 0.57. This indicates values of 0.94 and 14.34 for m and a, respectively. Dotted line is the best fit line that is forced to intercept y-axis at $\phi=1$ ($\log\phi = 0$) and $F = 1$ ($\log F = 0$). The slope of this line is -1.95 indicating a value of 1.95 for m, and 1 for a.

Scattering of the data in Figure 2, leading to small coefficient of determination (R^2=0.57), represent heterogeneities of the samples. Therefore, m and a derived from these methods are imprecise. Many studies have been carried out to classify rocks based on their lithology, facies, porosity type and permeability to achieve a better correlation between porosity and F (e.g. Focke and Munn, 1987; Byrnes et al., 2003).

5. Results and Discussions on the Classification Methods

In the following sections different classifications have been applied for the samples to find more accurate relationship between porosity and F.

5.1 Classification based on Petrofacies

In order to obtain more accurate correlation between porosity and F, the studied samples were classified based on their petrofacies. Figure 3 shows the cross-plot of porosity versus F for different petrofacies. Some petrofacies appear in narrower trends and show higher R^2 values. Table 3 presents the power law free best fit line equation, m, a, R^2 and the number of samples for each petrofacies. Free best fit line equations provided unusual values of m and a for most of the petrofacies. Forced best fit line provides more usual values for m (Table 3, last column).

5.2 Classification Based on Permeability and Petrofacies-Permeability Groups

Samples were classified based on their permeability classes to evaluate the effect of permeability on the ϕ-*F* plot. The permeability classes were defined as: K<1mD, 1<K<5, 5<K<10; 10<K<50 and K>50mD. Figure 4 shows the cross-plot of porosity versus *F* for each class of permeability. Although the classes were plotted separately to some extent, but a well defined fit line could not be obtained for each class using this method. This may be due to a weak relationship between *F* and permeability. Cross-plot of permeability versus *F* shows a weak correlation (Figure 5). For example samples with permeability of 20mD show *F* values of 30 to 526. This suggests that although there are many common parameters in hydraulic and electrical conductivity of porous media, but it seems other factors must be taken into account for carbonates with complex network of pores and pore throats.

5.3 Classification Based on Flow Zone Indicator

Generally, there is a weak correlation between porosity and permeability, especially in carbonates. To find a better correlation between porosity and permeability and define hydraulic flow unit (*HFU*), Amaefule et al. (1993) developed an expression as:

$$FZI = \frac{0.0314\sqrt{\frac{K}{\phi}}}{\phi_Z} \tag{20}$$

where *FZI*, *K* and ϕ are Flow Zone Indicator (μm), permeability (mD) and porosity (fraction), respectively. ϕ_Z is pore to matrix volume ratio (*PMR*) and can be expressed as:

$$\phi_Z = \frac{\phi}{1-\phi} \tag{21}$$

The equation defines a relationship between volume of void space (ϕ/1-ϕ) and its geometric distribution ($\sqrt{K/\phi}$). A hydraulic flow unit with identical hydraulic properties shows close *FZI* values. On a semi-log plot of permeability versus porosity, samples with similar *FZI* values normally plot together indicating close relationship between porosity and permeability in each *HFU*.

In the present study, *FZI* values were used for classification of the samples. The value for each sample was calculated using Equation 20. Log *FZI* was applied to separate different *HFUs*. The samples were grouped in four *HFUs* using four *FZI* classes (*FZI*>0.5, 0.5>*FZI*>0, 0>*FZI*>-0.5 and -0.5>*FZI*>-1). Plotting porosity versus permeability regardless of the sample classification resulted in scattered plot and low determination coefficient (Figure 6). However, in the same cross-plot when data were grouped in separate *HFUs*, R^2 was significantly increased (Figure 7).

With the same *HFU* groups, samples were later plotted on the F-ϕ cross-plot (Figure 8). Scattered data in each *HFU* indicates that this approach was not also successful for binning porosity and *F* in well-defined groups.

In general, it can be stated that classification of samples based on permeability or *FZI* values is not successful. It is indicated that hydraulic and electrical path are not identical and hydraulic tortuosity is much larger than electrical tortuosity. This is a fact as permeability scales to a pore throat radii with a power of four and the electric conductivity scales to a pore throat radii with a power of two (David, 1993). A study by Zhang and Knackstedt (1995) on fluid-flow and electrical conductivity of three dimensional random porous medium at a microscopic level showed that hydraulic tortuosity is systematically larger than the electrical tortuosity, and can differ by as much as an order of magnitude at lower porosities. Another study by Slater and Lesmes (2002) indicated that permeability does not correlate with *F* in unconsolidated sediments. Another study by Hilfer and Manwart (2001) on three-dimensional computer tomographic image of Fontainebleau sandstone revealed that the permeability and *F* can differ significantly even in models with identical geometrical properties.

6. A New Method for Sample Classification

Like porosity and permeability, in log-log plot of porosity versus *F*, data may scatter significantly for a mixture of heterogeneous rocks. This will lead to small R^2 and thus less reliable values for derived *m* and *a*. As discussed in previous sections, different approaches did not improve correlation between the data.

Combining Poiseuille's law for flow in cylindrical tubes, Darcy's law for fluid flow in a porous media and Kozeny-Carman model (1937), Amaefule et al., (1993) defined reservoir quality index (*RQI*) as:

$$RQI = 0.0314\sqrt{\frac{K}{\phi}} \tag{22}$$

where *RQI* is in μm, *K* is permeability (mD), ϕ is porosity (fraction) and 0.0314 is the conversion factor from mD to μm. *RQI* is an estimation of mean hydraulic pore throat radius. In a given porosity, an increase in mean hydraulic radius will increase permeability. In the other word, higher *RQI* values indicate better reservoir quality.

Although, a global relationship has not been found between permeability and *F*, an inverse proportionality has been reported by many authors (Wong et al.,1984; Guyon et al., 1987; Kostek et al.,1992; Nettelbladt et al., 1995; Celzard and Marêché, 2002). Taking this fact into account, an identical ratio to Equation 22 can be defined as:

$$ERI = \sqrt{\frac{\phi}{F}} \tag{23}$$

Since the ratio is an indication of electrical radius, it is called Electrical Radius Indicator (*ERI*). Unlike *RQI* which provides mean value of hydraulic radius, *ERI* is dimensionless and only quantitatively compares electrical radius of samples. Equation 23 shows that with a given ϕ, a decrease in *F*, will increase *ERI* and vice versa. A comparison of *RQI* and *ERI* represents a relatively good match in terms of data fluctuation (Figure 9), suggesting that both of them may address the same properties.

Lack of exact match between *RQI* and *ERI* values supports other studies findings (Zhang and Knackstedt, 1995; Hilfer and Manwart, 2001; Slater and Lesmes, 2002) which have shown that hydraulic and electrical path are not identical

ERI is an indicator of electrical radius for each sample. In order to separate samples with similar electrical flow properties, *ERI* must be divided to volume of void space or pore to matrix volume ratio (ϕ/1-ϕ):

$$CZI = \frac{\sqrt{\frac{\phi}{F}}}{\phi_Z} \tag{24}$$

where ϕ, F and ϕ_Z are porosity (fraction), formation factor and pore to matrix volume ratio (*PMR*) respectively. The equation defines relation between the volume of void space (ϕ/1-ϕ) and its electrical flow properties ($\sqrt{\phi}/F$). The equation has been able to separate samples with similar electrical flow properties, and for this reason it is named "Current Zone Indicator" (*CZI)*. *CZI* is a factor that can be used to separate samples with relatively identical *m* and *a,* where the variation in *F* is just the function of porosity. Electrical flow unit (*EFU*), units with the same electrical flow properties, has been proposed for any samples that fall within a defined range of *CZI*. It is obvious that a homogenous interval of a reservoir with similar electrical flow properties will show close *CZI* values. Such an interval is a unit that has identical electrical flow properties that is named here as an *EFU*.

Equation 24 was used to calculate the *CZI* value for each sample in this study. The *CZI* values ranged from 0.43 to 0.12 with an average of 0.26. Four *EFUs* were defined using four *CZI* classes including CZI>0.3, 0.3>CZI>0.25, 0.25>CZI>0.20, *CZI*<0.20.

Figure 10 shows the cross-plot of porosity versus *F* binned in four *CZI* classes. The main difference between each *EFU* was the amount of isolated vuggy and/or moldic porosity. From *EFU1* to *EFU4* the number of isolated pores increases. This suggests that, increase in tortuosity from *EFU1* to *EFU4* is not due to porosity reduction. Higher tortuosity of pore throat networks is due to presence of isolated and dead-end pores which in turn lead to a longer pathway.

Table 4 lists *CZI* classes, power law best fit line equation, *m*, *a* and R^2 between porosity and *F* in each *EFU*. With this approach, R^2 has been increased significantly which in turn enables us to obtain more reliable *m* and *a*.

7. Comparison of *F* derived from different methods

In this study different methods provided different values for *m* and *a*. A free best fit line indicated *m*=0.94 and *a*=14.34, and a forced fit line with *a* =1, showed a value of 1.95 for *m* (Figure 2). Classification of the samples based on their *CZI* values also revealed different *m* and *a* (Table 4). Formation factor was calculated for each sample using

Equation 3, with *m* and *a* values derived from the three methods. Calculated *F* was then plotted against measured *F* (Figure 11). A significantly better R^2 (0.95) was achieved using *CZI* method.

8. Water Saturation Calculation Sensitivity Using Different Methods

In this section, the influence of *m* and *a* on *Sw* calculation using different methods will be discussed. With a fixed *a (a* =1) the slope of the best fit line increases comparing to the free best fit line (Figure 2). Using Equation 13, if *m* changes from *m1* (1.1, 1.18, 1.22 and 1.34, Table 4) to *m2*=1.95, then *a* must be adjusted to achieve the same *F* value for each sample. In the other word, when *m* is considered 1.95, the calculated *a* values must be used instead of *a* =1 to obtain accurate *F*. Figure 12 shows histogram of calculated *a* values from Equation 13. It shows that about 14% of *a* values are close to 1, 56% are higher than 1.15 and 30% are lower than 0.9.

Figure 13 compares *F* values obtained from forced and *CZI* methods. According to Equation 4, *F* has direct relation with *Sw* in a given *Rw* and *Rt*. Where *a* values depart from 1, calculated formation factors from two methods depart form each other progressively (Figure 13). With *a* values of larger than 1, 56% of calculated *F* from forced method shows lower values comparing to *CZI* method (left part of Figure 13) resulting in underestimation of *Sw*. When *a* values are less than 1, 30% of *F* from forced method show higher values (right part of Figure 13) leading to *Sw* overestimation. Only 14% of calculated *F* values from forced method are valid and gain correct *Sw* for the studied samples.

In the meanwhile, *F* values calculated from the free method does not match the *F* values from *CZI* method (Figure 14). The small correlation between porosity and *F* (Figure 2) has led to small fit between these values.

9. Conclusion

This study shows that for heterogeneous carbonates with microscopically complex pore networks the relation between *F* and porosity is not straightforward. For such complex reservoirs, using a unique value for *m* and *a* will lead to an inaccurate estimation of hydrocarbon reserves.

The most basic and widely used form of Archie's equation for carbonates is:

$$F = \frac{1}{\phi^2} \tag{25}$$

Although, an assumed $m = 2$ and $a = 1$ is relatively fair choice for carbonates with dominantly interparticle and intercrystalline porosity, for carbonates with secondary porosity and complex network of pores and pore throat however it may cause a significant error in *Sw* estimation.

This study shows that classification of rocks based on petrofacies, permeability and *FZI* is inadequate to obtain accurate values for *m* and *a*. In additions, using free best fit line without sample classification and or fixing *a* to a constant value, which causes *m* to increase, may lead to both over and underestimation of *Sw*.

Application of *CZI* method to classify the samples in well defined groups (*EFUs*) provided a suitable method to obtain accurate *a* and *m* and thus better estimation of *Sw*. *CZI* method has shown that the samples fall into multiple groups where the variation is mostly due to tortuosity factor. For each group, unlike *m* that vary slightly from 1.1 to 1.3, *a* changes from 5 to 19. The wide variation of *a* from *EFU1* to *EFU4* is mostly due to an increase in the isolated and dead-end pores. This study suggests, unlike rocks with intergranular and well-connected pores, for rocks with complex pore networks where most of the intergranular pores are occluded by cements and irregularly-distributed secondary pores are either isolated or connected by tortoise path, tortuosity plays an important role controlling electrical conductivity.

This suggests that, increase in tortuosity from *EFU1* to *EFU4* is not due to porosity reduction. Higher tortuosity of pore throat networks is due to presence of isolated and dead-end pores which in turn lead to a longer pathway.

Acknowledgements

The authors are grateful for financial support by the NIOC - Research & Development Directorate, the University of Tehran and Research Institute of Petroleum Industry (RIPI). Mr. M. Rahimi and K. Saadat are acknowledged for conducting lab tests. We thank Dr. S. Etemadi for critical review of the article. The authors acknowledge NIOC - Research & Development Directorate for permission to publish this paper.

References

Archie, G.E., 1942. The electrical resistivity log as an aid in determining some reservoir characteristics. Trans. Am. Inst. Min. Metall. Pet. Eng., 146:54-62.

Winsauer, W.O., Shearin, H.M., Masson, P.H., and Williams, M., 1952. Resistivity of brine -saturated sands in relation to pore geometry. AAPG Bulletin, 36:253-277.

Timur, A., Hempkins, W.B., Worthington, A.E., 1972. Porosity and pressure dependence of formation resistivity factor for sandstones. Presented at Form. Eval. Symp. Can. Well Log. Soc., 4th, Calgary (Paper, D).

Wong P-Z., Koplik J., and Tomanic J.P., 1984. Conductivity and permeability of rocks. Phys. Rev. B, 30:6606-6614

Focke, J.W., and Munn D., 1987. Cementation exponents in middle eastern carbonate reservoirs. SPE Formation Evaluation, 2:155-167.

Neustaedter, R.H., 1968, Log evaluation of deep Ellenburger gas zones. SPE Paper 2071, presented at the Deep Drilling and Development Symposium-Delaware Basin of the SPE of AIME, Monahans, Texas.

Nugent, W.H., Coates, G.R., and Peebler, R.P., 1978. A new approach to carbonate analysis.19th SPWLA Symposium, Paper O.

Sethi, D.K., 1979. Some considerations about the formation resistivity factor-porosity relations. 20th SPWLA Symposium, paper L.

Rasmus, J.C., 1983. A variable cementation exponent, *m*, for fractured carbonates. The Log Analyst, 24:13-23.

Borai, A.M., 1987. A new correlation for the cementation factor in low-porosity carbonates. SPE Formation Evaluation, 2:495-499.

Carman, P.C., 1937. Fluid flow through granular beds. Transactions of the Institute of Chemical Engineers, 15:150-167.

Bird, R.B., Stewart, W.E., and Lightfoot, E.N., 1960. Transport Phenomena. John Wiley & Sons, New York.

Wyllie, M.R.J., and Rose, W.D., 1950. Some theoretical considerations related to the quantitative evaluation of the physical characteristics of reservoir rock from electrical log data. Transactions of AIME, 189:105-118.

Salem, H.S., and Chilingarian, G.V., 1999. The cementation factor of Archie's Equation for shaly sandstone reservoirs. Journal of Petroleum Science and Engineering, 23:83-93.

Amaefule, J.O., Altunbay, M., Tiab, D., Kersey, D.G., and Keelan, D.K., 1993. Enhanced reservoir description: Using core and log data to identify hydraulic (flow) units and predict permeability in uncored intervals/wells. SPE Paper 26436, 1–16.

David, C., 1993. Geometry of flow path for fluid transport in rocks. Journal of Geophysical Research, 98: 12267-12278.

Zhang, X., and Knackstedt, M.A., 1995. Direct simulation of electrical and hydraulic tortuosity in porous solids. Geophysical Research Letters, 22:2333–2336.

Guyon E., Oger L., and Plona TJ., 1987. Transport properties in sintered porous media composed of two particle sizes. J. Phys. D: Appl. Phys., 20:1637-1644.

Kostek S, Schwartz L.M., and Johnson D.L., 1992. Fluid permeability in porous media: Comparison of electrical estimates with hydrodynamical calculations. Phys. Rev. B, 45:186-95

Nettelbladt, B., Ahlent, B., Niklassons, G.A., and Holtll, R.M., 1995. Approximate determination of surface conductivity in porous media. J. Phys. D: Appl. Phys., 28:2037-2045.

Hosseini-nia, T., and Rezaee, M.R., 2002. Error sensitivity of petrophysical parameters on water saturation calculation for hydrocarbon reservoirs. J. Sci. Univ. Tehran, 28:69-91.

Hamada, G.M., Al-Awad, M.N.J., and Alsughayer, A.A., 2002. Water saturation computation from laboratory, 3D Regression. Oil & Gas Science and Technology – Rev. IFP, 57:637-651.

Dubois, M.K., Byrnes, A.P., and Watney, W.L., 2001. Field development and renewed reservoir characterization for Co_2 flooding of the Hall-Gurney Field, Central Kansas. AAPG Annual Convention in Denver, Colorado.

Hirasaki, G.J., Flow and Transport Through Porous Media, Course note.

Attia M.A., 2005. Effects of petrophysical rock properties on tortuosity factor. Journal of Petroleum Science and Engineering, 48:185-198.

Maghsoodi, F., Rezaee, M.R., 2005. Effects of microfacies, sedimentary environment and digenesis on the reservoir quality of the Asmari Formation, Gachsaran Field, 9th Geological Society of Iran Conference, 683-698.

Byrnes, A.P., Franseen, E.K., Wateney, W.L., and Dubois, M.K., 2003. The role of moldic porosity in paleozoic kansas reservoirs and the association of original depositional facies and early diagenesis with reservoir properties. AAPG Annual Convention in Salt Lake City, Utah.

Slater, L., and Lesmes, D.P., 2002. Electrical-hydraulic relationships observed for unconsolidated sediments, Water Resources Research, 38:31-1.

Hilfer R., and Manwart, C., 2001. Permeability and conductivity for reconstruction models of porous media. Physical Review E, 64:021304.

Celzard, A., and Marêché, J.F., 2002. Fluid flow in highly porous anisotropic graphites. Journal of Physics: Condensed Matter, 14:1119-1129

Tables 1 to 4
Click here to download Table: Tables.doc

Table 1 – Formation factors for different values of porosity, m and a.

	Porosity (fraction)				
	0.05	**0.10**	**0.20**	**0.30**	**0.40**
F1 (m_1=1.8 and a_1=1.2)	263.655	75.715	21.743	10.480	6.244
F2 (m_1=1.9 and a_1=1.5)	444.681	119.149	31.925	14.776	8.554
F3 (m_1=2.2 and a_1=1.4)	1019.516	221.885	48.291	19.791	10.510
F4 (m_1=2.4 and a_1=1.3)	1723.516	326.545	61.869	23.380	11.722
F5 (m_1=2.6 and a_1=1.2)	2896.405	477.729	78.796	27.458	12.996
F6 (m_1=3 and a_1=1)	8000.000	1000.000	125.000	37.037	15.625

Table 2 – Calculated tortuosity factor (a_2) using F values in Table 1.

$a_2 = F\phi^2$	Porosity (fraction)					Equations
	0.05	**0.10**	**0.20**	**0.30**	**0.40**	
a_2 for $F1$	0.659	0.757	0.870	0.943	0.999	$a_2 = 1.2\phi^{0.2}$
a_2 for $F2$	1.112	1.191	1.277	1.330	1.369	$a_2 = 1.5\phi^{0.1}$
a_2 for $F3$	2.549	2.219	1.932	1.781	1.682	$a_2 = 1.4\phi^{-0.2}$
a_2 for $F4$	4.309	3.265	2.475	2.104	1.876	$a_2 = 1.3\phi^{-0.4}$
a_2 for $F5$	7.241	4.777	3.152	2.471	2.079	$a_2 = 1.2\phi^{-0.6}$
a_2 for $F6$	20.000	10.000	5.000	3.333	2.500	$a_2 = 1\phi^{-1}$

Table 3 - Free best fit line equations, m, a, R^2 and number of samples for seven petrofacies. Sandy Dolostone due to very small sample size (2 samples) was excluded. Last column shows m values using forced fit method for each petrofacies.

Petrofacies	Equations	m	a	R^2	No.	m (from forced method)
Dolomicrite	$F = 5.22\phi^{-1.11}$	1.11	5.22	0.97	3	2.03
Mudstone	$F = 0.5\phi^{-2.4}$	2.4	0.5	0.90	5	2.14
Grainstone	$F = 22.56\phi^{-0.74}$	0.74	22.56	0.87	10	1.77
Packstone	$F = 12.53\phi^{-0.94}$	0.94	12.53	0.75	14	1.84
Dolomitized packstone-grainstone	$F = 49.5\phi^{-0.55}$	0.55	49.5	0.66	16	1.87
Dolostone	$F = 12.58\phi^{-0.1.03}$	1.03	12.58	0.56	36	2.08
Wackstone	$F = 14.8\phi^{-1.02}$	1.02	14.8	0.31	6	2.21

Table 4 – Summary of data obtained from Figure 10.

EFU	CZI Class	Equation	m	a	R^2
1	CZI>0.3	$F=5.58\phi^{-1.1}$	1.10	5.58	0.97
2	0.3>CZI>0.25	$F=7.01\phi^{-1.18}$	1.18	7.01	0.96
3	0.25>CZI>0.2	$F=9.35\phi^{-1.22}$	1.22	9.35	0.96
4	CZI<0.2	$F=14.19\phi^{-1.34}$	1.34	14.19	0.85

Figures Captions

Figure 1 - Cross-plot of porosity versus tortuosity factor (data from Table 2). For samples with $m_1<m_2$, (a_2 for F_1 and a_2 for $F2$), with an increase in porosity, tortuosity factor increases. For samples with $m_1>m_2$, (a_2 for $F3$ to a_2 for $F6$) tortuosity factor decreases with an increase in porosity. In both cases variation of tortuosity factor is to keep the F values of Table 1 unchanged.

Figure 2 - Log porosity versus log F. Forcing fit line to intercept y-axis at a=1 and F=1, has led to a higher value for m.

Figure 3 - Log-log plot of porosity versus formation factor for eight petrofacies. Some of the petrofacies such as grainstone and packstone show a narrower and relatively well defined trend. Dolostone samples are scattered on the plot.

Figure 4 – Log-log plot of porosity versus formation factor. Samples in this plot are separated based on permeability classes.

Figure 5 - Cross-plot of permeability versus formation factor. An inverse relationship exists between F and permeability. In general the relationship is poor and R^2 is 0.25.

Figure 6 – Semi-log cross-plot of porosity versus permeability for the samples. The determination coefficient is 0.59.

Figure 7 - The same cross-plot of Figure 6, but data were grouped in four hydraulic flow units (*HFUs*). Note the large R^2 values for each *HFU*.

Figure 8 - Log-log plot of porosity versus formation factor. The samples are classified based on *FZI* values into four *HFUs*. There is no clear separation for each *HFU* on the plot.

Figure 9 - A comparison between *RQI* and *ERI*. For most of the samples there is a good match between *RQI* and *ERI*. Note that scales are different.

Figure 10 - Log-log plot of porosity versus formation factor. Samples have been grouped in four electrical flow units (*EFUs*) based on their *CZI* values.

Figure 11 - Comparison of measured *F* with calculated *F* from *CZI* (A), free (B) and forced (C) methods. Obtained *m* and *a* values from *CZI* resulted in more accurate values for *F*.

Figure 12 - Histogram showing variations of calculated tortuosity factor using equation 13 for the studied samples. For most of the samples the tortuosity is larger or smaller than 1.

Figure 13 - A comparison of formation factors calculated from forced and *CZI* methods. As calculated tortuosity factor (bars at the top of the figure) departure from 1, *F* values calculated from two methods depart from each other. When $a>1$ (left side of figure) *F* from forced method generally shows smaller values. When $a<1$ (right side of figure) *F* from forced method show larger values.

Figure 14 - A comparison between formation factors calculated from free, forced and *CZI* methods. *F* calculated from free method varies considerably and do not match with *F* derived from *CZI* method.

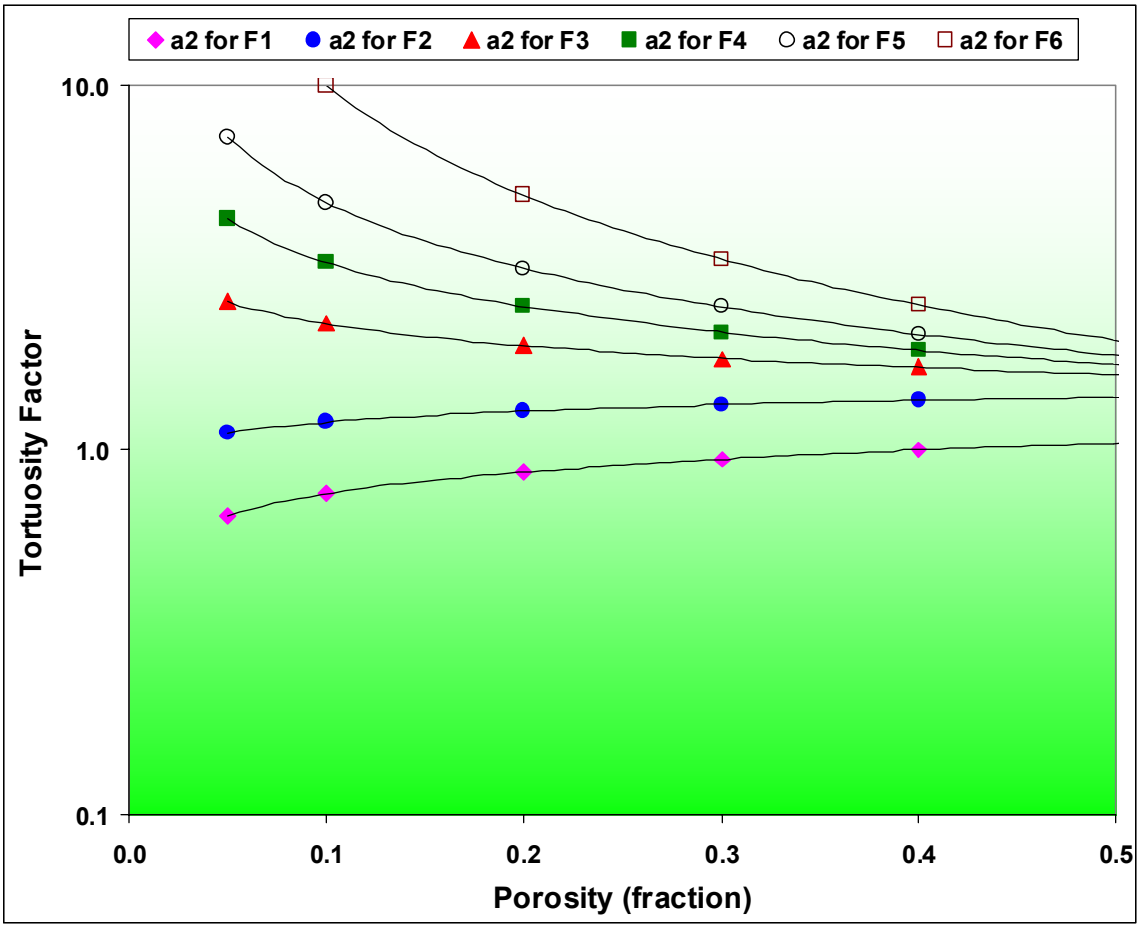
a2 for F1
a2 for F2
a2 for F3
a2 for F4
a2 for F5
a2 for F6
10.0
1.0
0.1
Tortuosity Factor
0.0
0.1
0.2
0.3
0.4
0.5
Porosity (fraction)

Figure 1

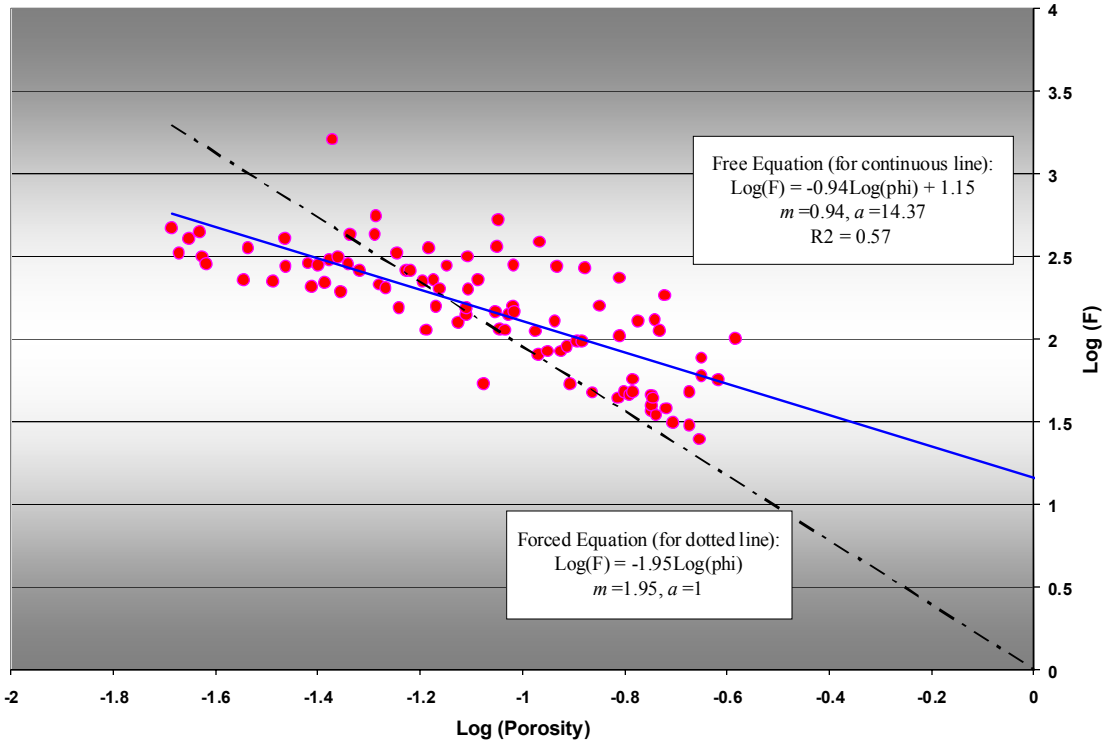
Free Equation (for continuous line):
Log(F) = -0.94Log(phi) + 1.15
m =0.94, a =14.37
R2 = 0.57
Forced Equation (for dotted line):
Log(F) = -1.95Log(phi)
m =1.95, a =1
Log (F)
Log (Porosity)
4
3.5
3
2.5
2
1.5
1
0.5
0
-2
-1.8
-1.6
-1.4
-1.2
-1
-0.8
-0.6
-0.4
-0.2
0

Figure 2

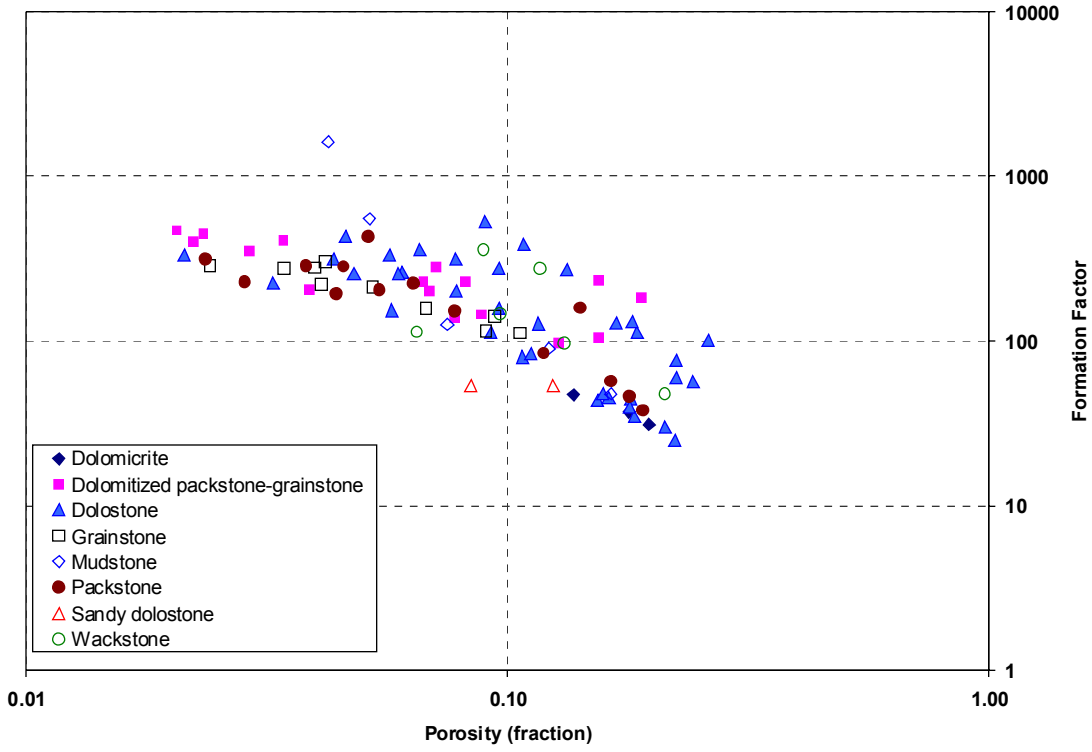
10000
1000
100
10
1
Formation Factor
0.01
0.10
1.00
Porosity (fraction)
Dolomicrite
Dolomitized packstone-grainstone
Dolostone
Grainstone
Mudstone
Packstone
Sandy dolostone
Wackstone

Figure 3

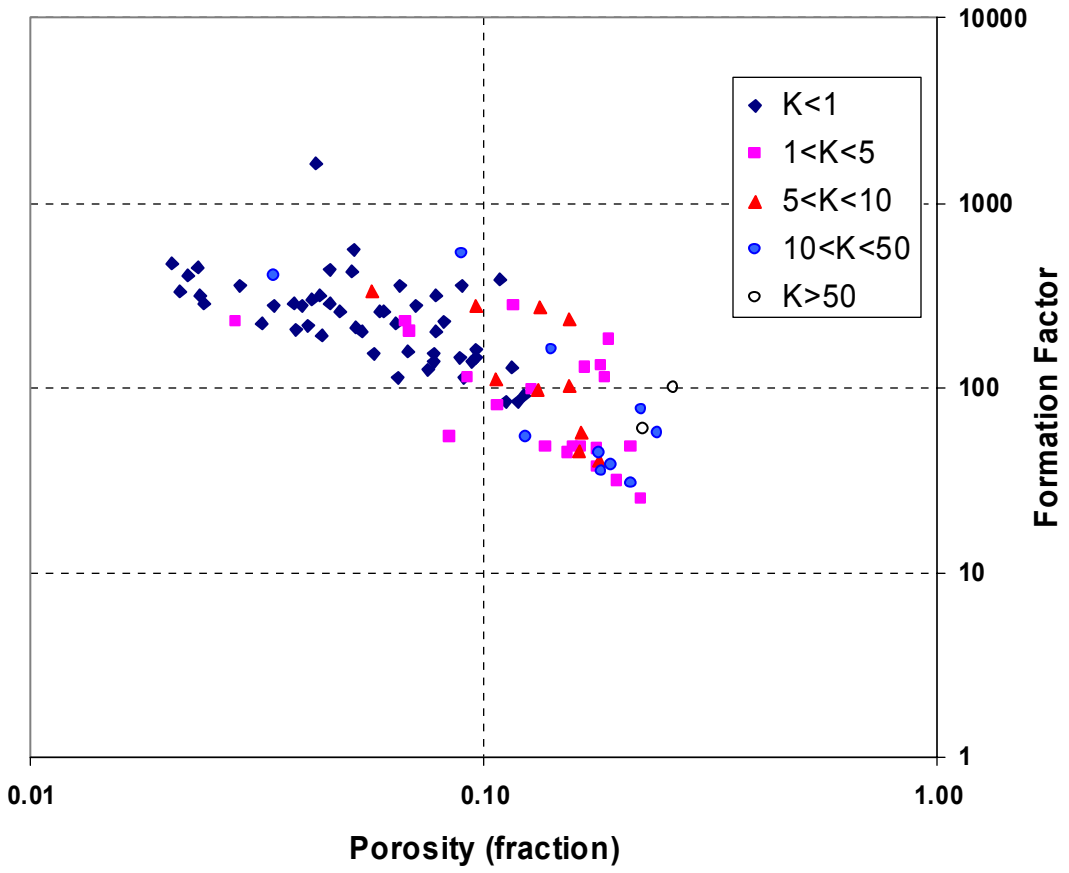
10000
1000
100
10
1
Formation Factor
K<1
1<K<5
5<K<10
10<K<50
K>50
0.01
0.10
1.00
Porosity (fraction)

Figure 4

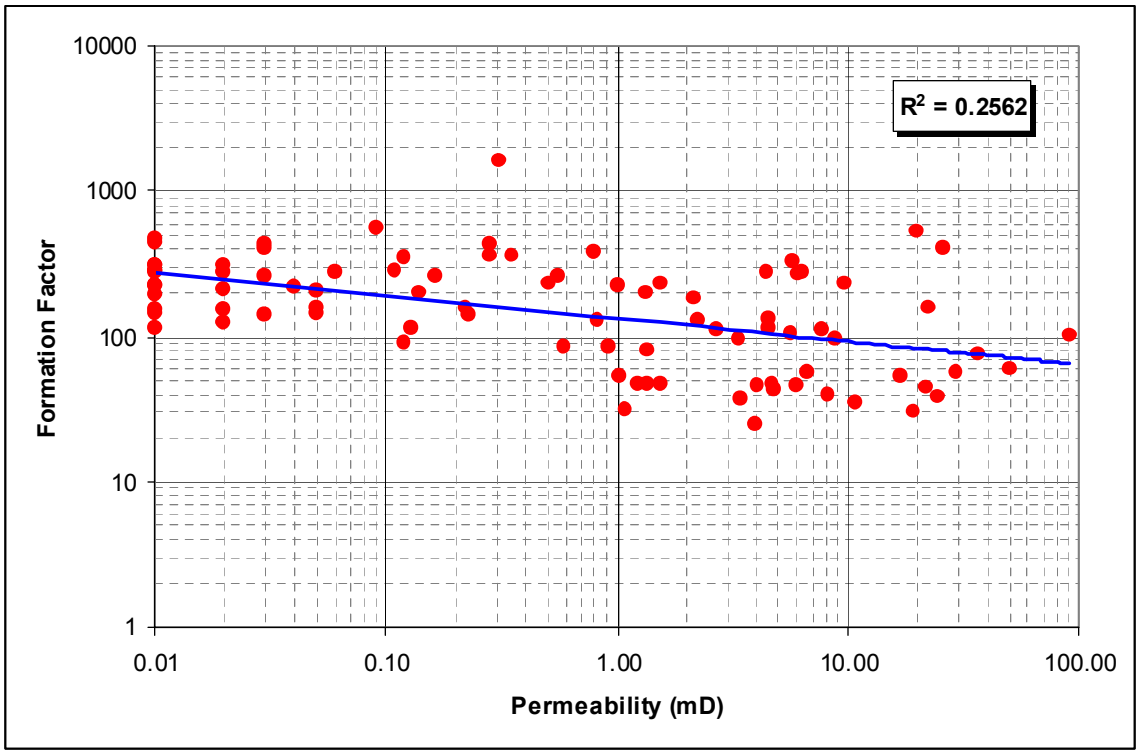
10000
1000
100
10
1
Formation Factor
0.01
0.10
1.00
10.00
100.00
Permeability (mD)
R2 = 0.2562

Figure 5

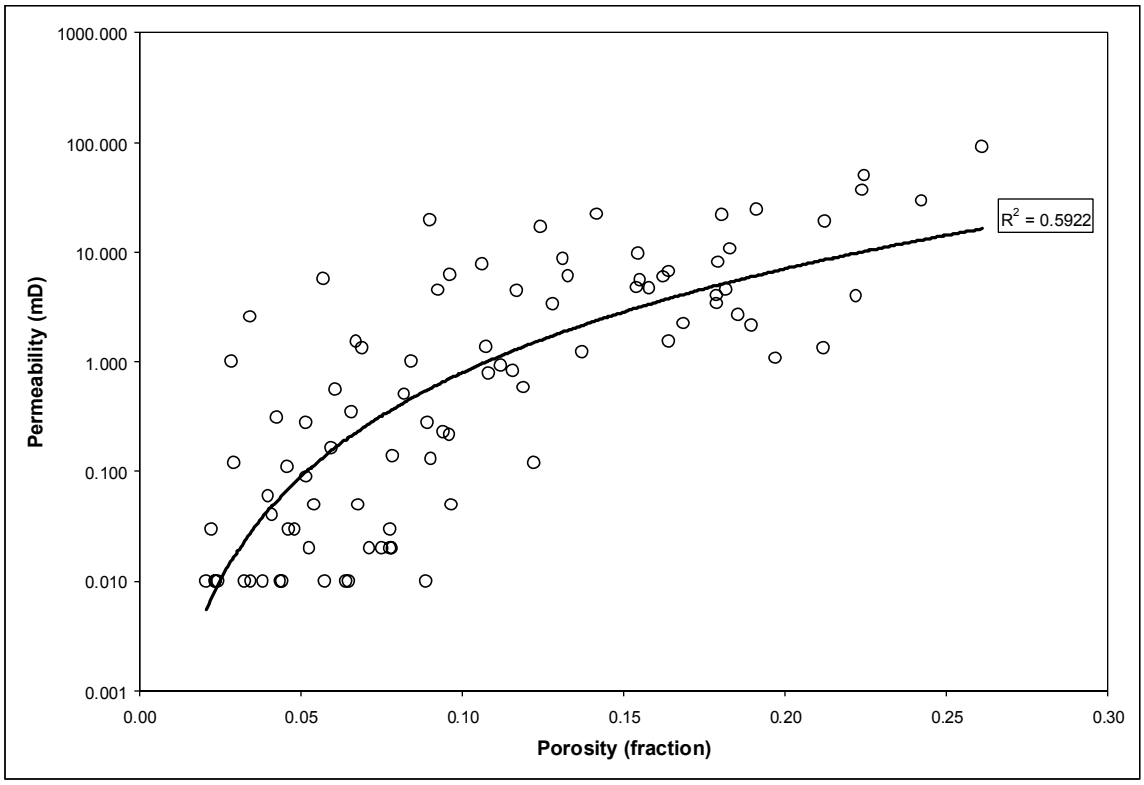
1000.000
100.000
10.000
1.000
0.100
0.010
0.001
Permeability (mD)
0.00
0.05
0.10
0.15
0.20
0.25
0.30
Porosity (fraction)
R2 = 0.5922

Figure 6

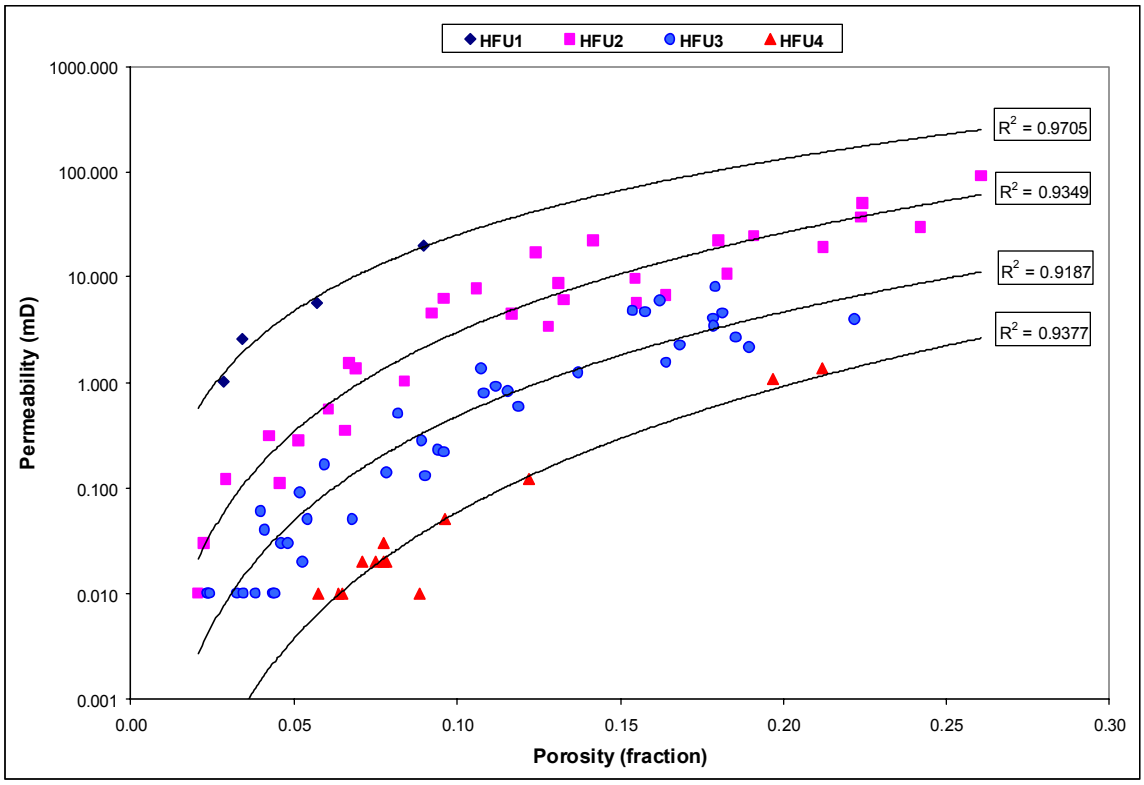
HFU1
HFU2
HFU3
HFU4
1000.000
100.000
10.000
1.000
0.100
0.010
0.001
Permeability (mD)
0.00
0.05
0.10
0.15
0.20
0.25
0.30
Porosity (fraction)
R2 = 0.9705
R2 = 0.9349
R2 = 0.9187
R2 = 0.9377

Figure 7

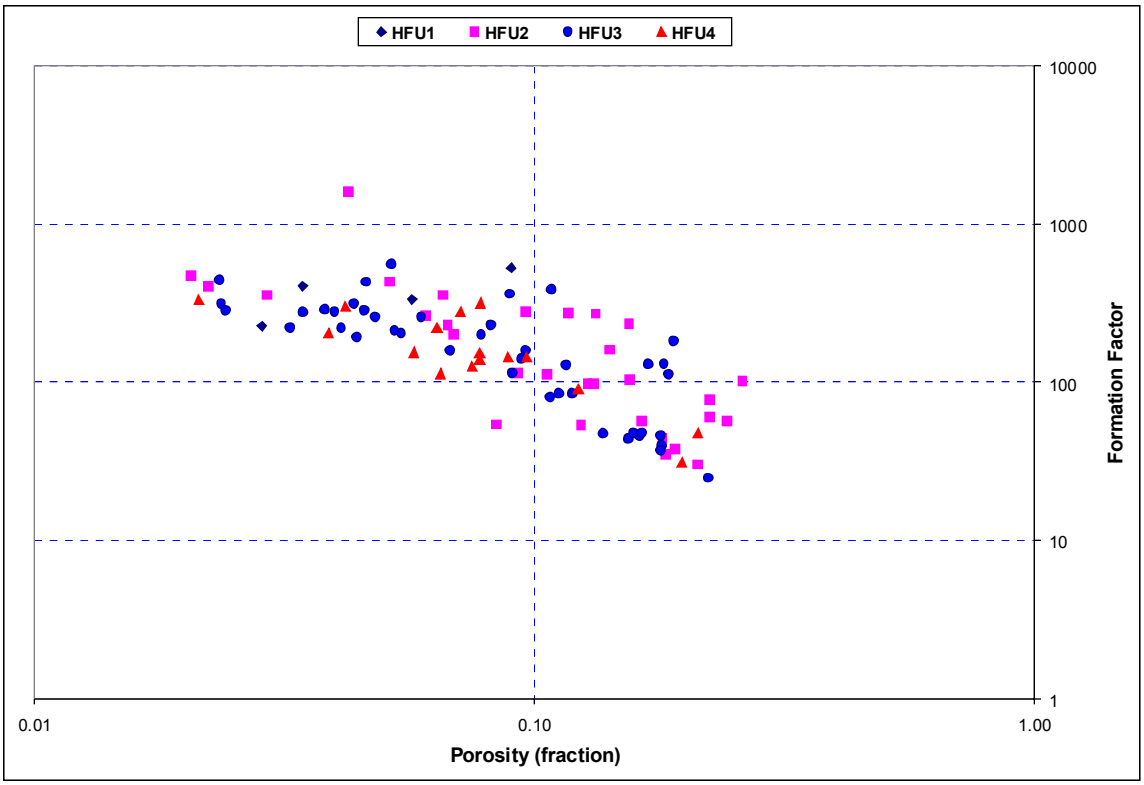
HFU1
HFU2
HFU3
HFU4
10000
1000
100
10
1
Formation Factor
0.01
0.10
1.00
Porosity (fraction)

Figure 8

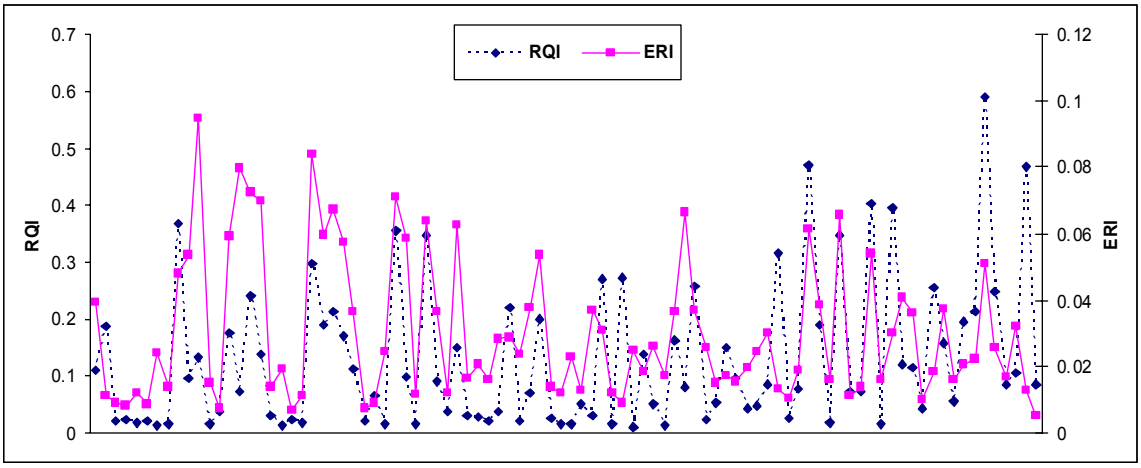

Figure 9

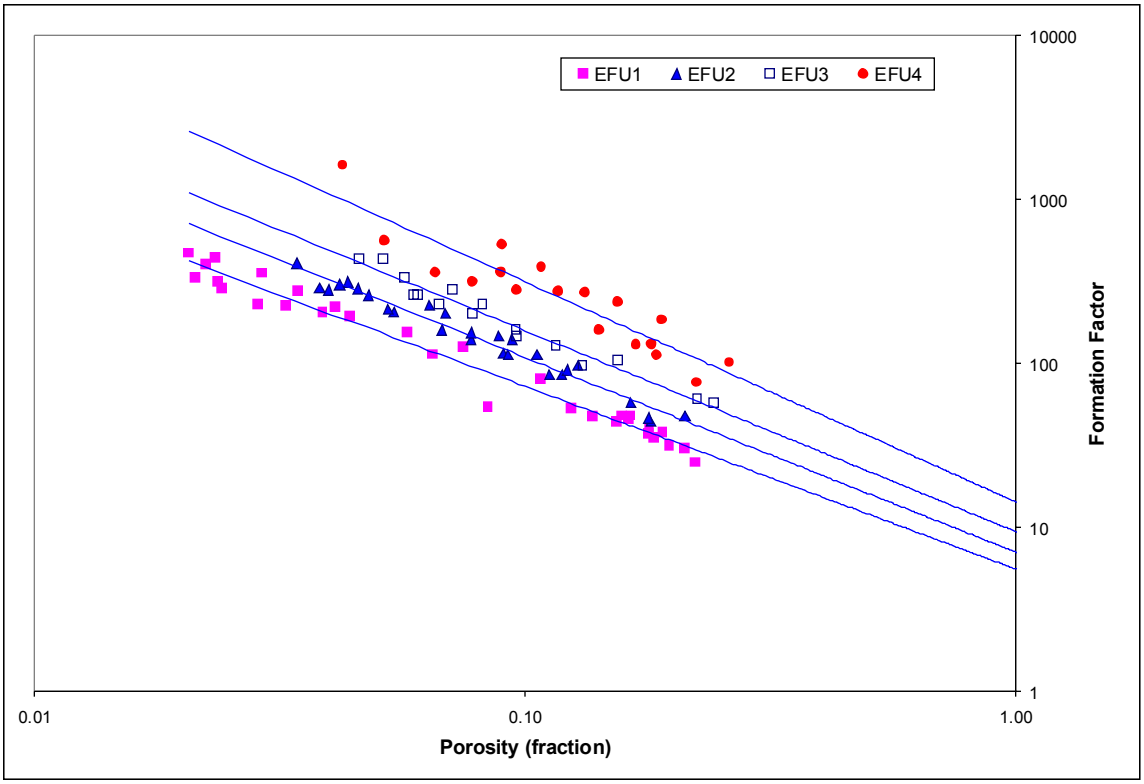
EFU1
EFU2
EFU3
EFU4
10000
1000
100
10
1
Formation Factor
0.01
0.10
1.00
Porosity (fraction)

Figure 10

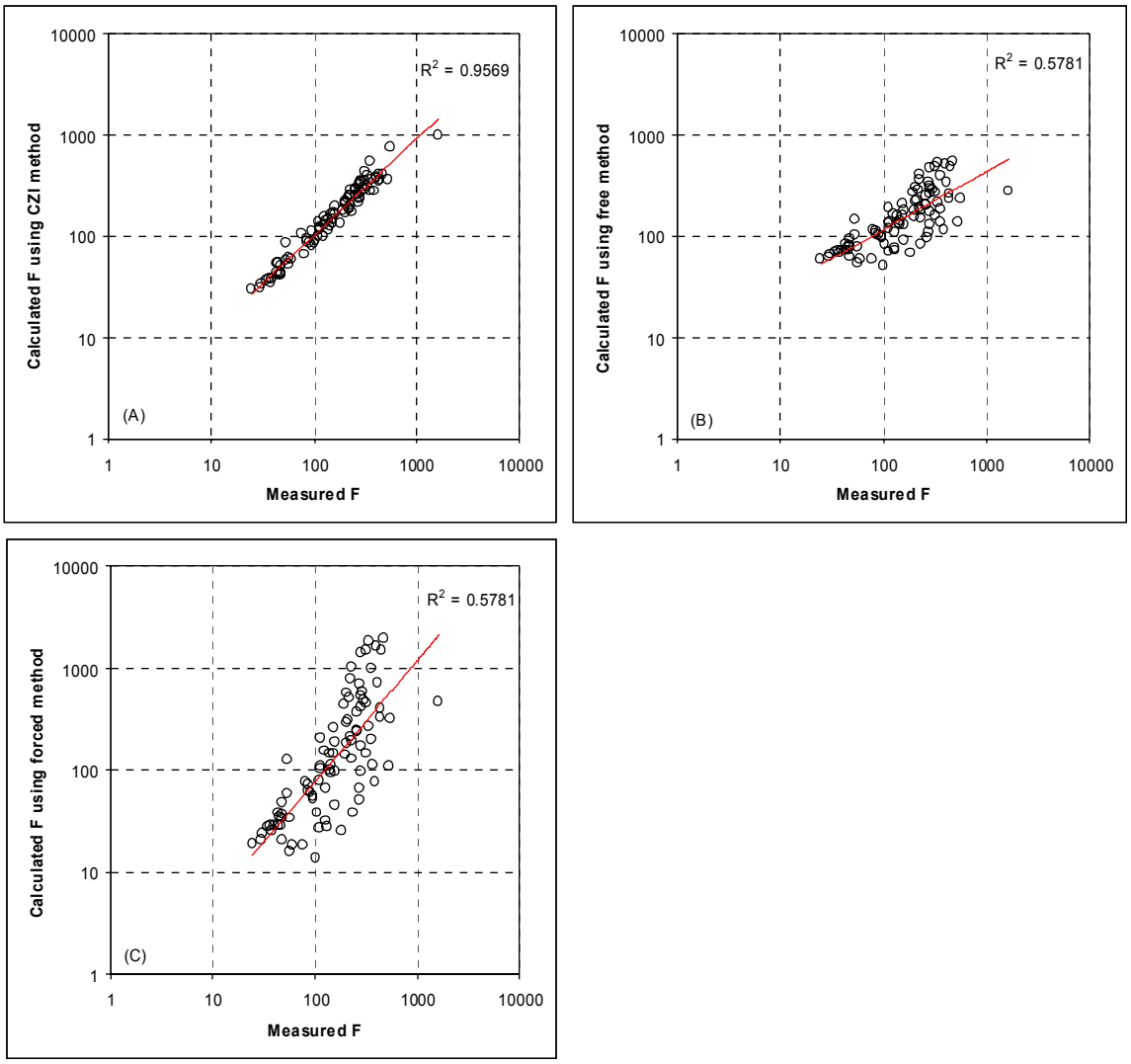
Calculated F using CZI method
Measured F
R^2 = 0.9569
(A)
Calculated F using free method
Measured F
R^2 = 0.5781
(B)
Calculated F using forced method
Measured F
R^2 = 0.5781
(C)
10000
1000
100
10
1
1
10
100
1000
10000

Figure 11

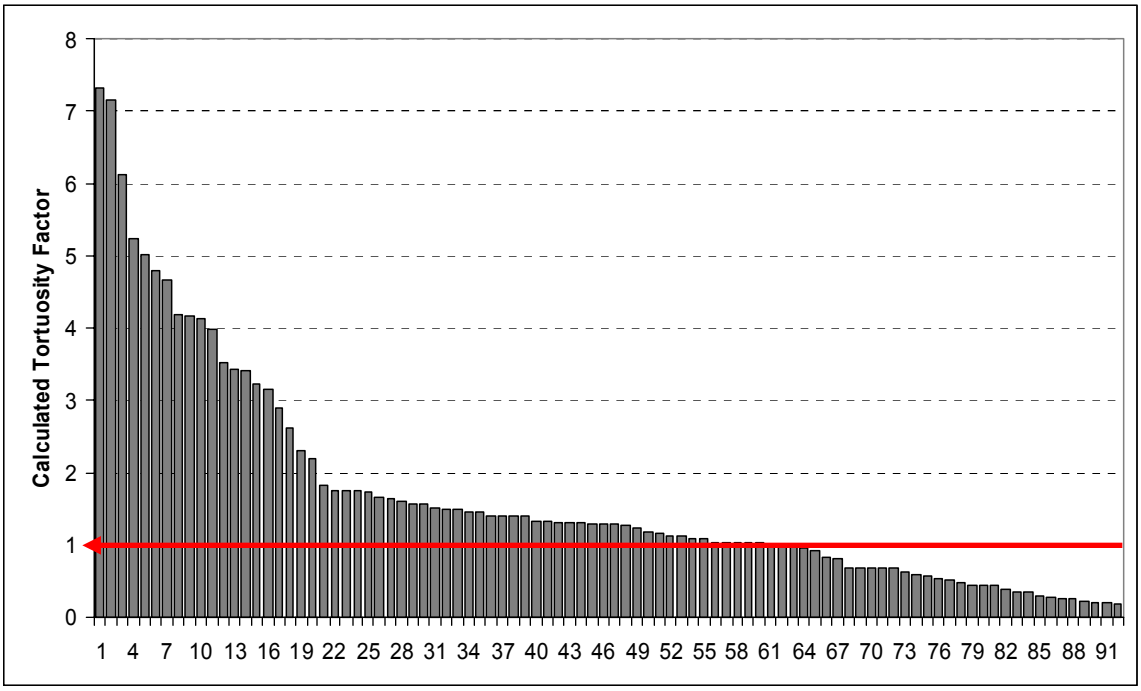
Calculated Tortuosity Factor
8
7
6
5
4
3
2
1
0
1 4 7 10 13 16 19 22 25 28 31 34 37 40 43 46 49 52 55 58 61 64 67 70 73 76 79 82 85 88 91

Figure 12

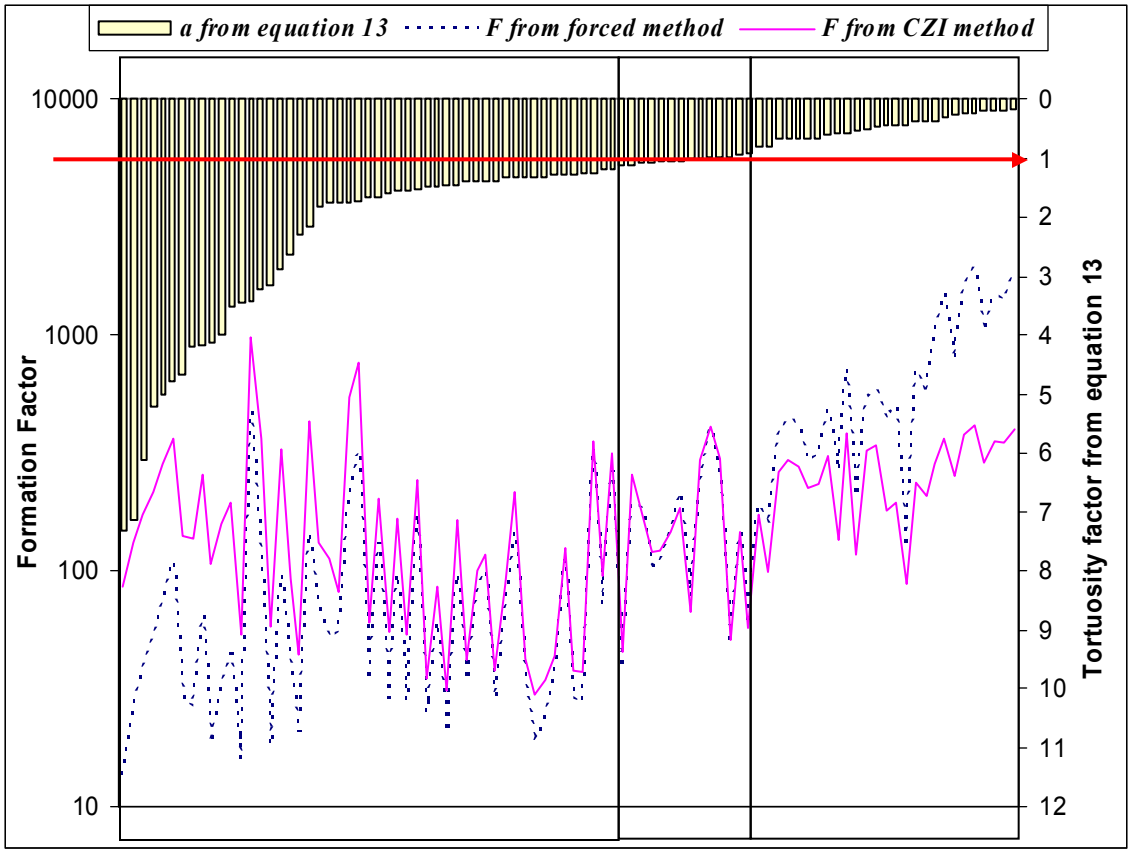
a from equation 13
F from forced method
F from CZI method
10000
1000
100
10
Formation Factor
0
1
2
3
4
5
6
7
8
9
10
11
12
Tortuosity factor from equation 13

Figure 13

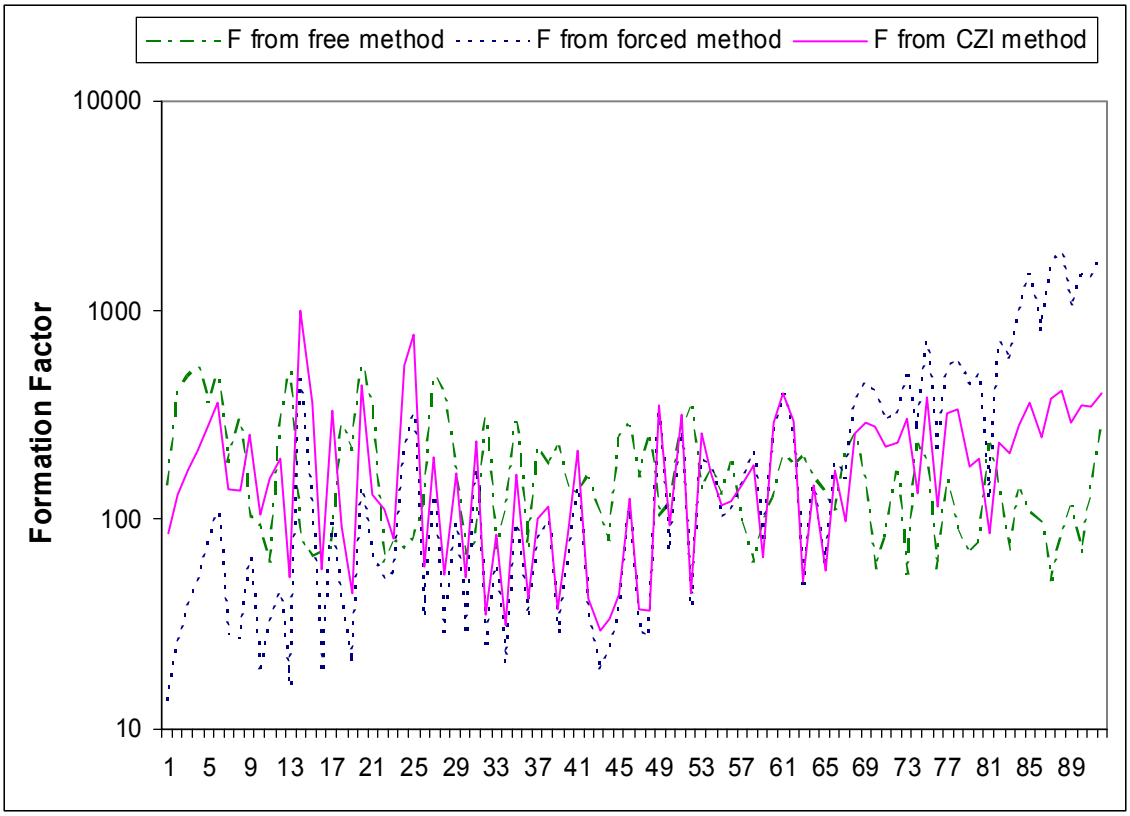
F from free method
F from forced method
F from CZI method
Formation Factor
10000
1000
100
10
1 5 9 13 17 21 25 29 33 37 41 45 49 53 57 61 65 69 73 77 81 85 89

Figure 14